Theoretical Studies of Inorganic and Organometallic Reaction Mechanisms. 15. Catalytic Alkane Dehydrogenation by Iridium(III) Complexes

Shuqiang Niu[†] and Michael B. Hall*

Contribution from the Department of Chemistry, Texas A&M University, College Station, Texas 77843

Received April 20, 1998. Revised Manuscript Received January 12, 1999

Abstract: Alkane dehydrogenation catalyzed by the Ir(III) complexes (PCP′)Ir(H)$_2$ (**1**) [PCP′ = η^3-$C_6H_3(CH_2PH_2)_2$-1,3] and CpIr(PH$_3$)(H)$^+$ (**10**) [Cp = η^5-C_5H_5] is investigated with density functional theory (DFT). For both systems the theoretical results show that catalytic alkane dehydrogenation to alkene proceeds through (i) alkane oxidative addition, (ii) dihydride reductive elimination, (iii) β-H transfer from alkyl ligand to metal, and finally (iv) elimination of the olefin. Barriers for steps (i), (ii), and (iv) are critical for the catalytic cycle. The (PCP′)Ir(H)$_2$ system is special because these three barriers are balanced (16, 15, and 22 kcal/mol, respectively), whereas in the CpIr(PH$_3$)(H)$^+$ system these three barriers are unbalanced (9, 24, and 41 kcal/mol, respectively). Thus, in the catalytic cycle for alkane dehydrogenation by (PCP′)Ir(H)$_2$ the reaction endothermicity is achieved gradually. The higher stability of the formally Ir(V) complexes and the η^2-alkene complex, which has some Ir(V)-like character, in the CpIr(PH$_3$)(H)$^+$ system is responsible for the larger barriers in these critical steps. In the key role played by the ligand systems, PCP′(H) *vs* Cp(PH$_3$), the former increases the energy of the metal−ligand fragment's triplet state relative to that of the singlet and thus destabilizes all the Ir(V)-like species.

Introduction

Alkane dehydrogenation catalyzed by transition-metal complexes is an important goal for organometallic chemistry (reaction 1).[1]

$$\text{alkanes} \xrightarrow{\text{cat.}} \text{alkenes} + H_2 \qquad (1)$$

The dehydrogenation of alkanes to produce alkenes, in addition to being highly endothermic (experimentally about 33 kcal/mol), is a symmetry-forbidden reaction and has an extremely high barrier without a catalyst.[2] Thus, the reaction usually proceeds only under UV irradiation or in the presence of a hydrogen acceptor. Even with a catalyst, the reaction still requires energy and typically occurs only at higher temperatures.[3]

In early work, Crabtree and co-workers described an Ir(III) system, Ir(H)$_2$(Me$_2$CO)(PPh$_3$)$_2^+$, that thermally dehydrogenates cyclopentenes to cyclopentadienyl complexes.[4] Recently, Bergman and co-workers reported another Ir(III) system, Cp*Ir(PMe$_3$)(CH$_3$)$^+$ [Cp* = η^5-$C_5(CH_3)_5$], that thermally activates alkanes in the solution phase at unprecedentedly low temperatures to generate olefin complexes.[5] Recent density functional theory (DFT) calculations suggest that the reaction of CpIr(PH$_3$)(CH$_3$)$^+$ with an alkane proceeds through oxidative-addition (OA) of the alkane, reductive-elimination (RE) of methane, and β-H transfer to form CpIr(PH$_3$)(H)(η^2-alkene)$^+$. The overall reaction is exothermic by about 15 kcal/mol.[6] Most recently, Kaska, Jensen, and co-workers describe an iridium(III) catalytic system, (PCP)Ir(H)$_2$ [PCP = η^3-$C_6H_3(CH_2PBu^t_2)_2$-1,3], that catalyzes the dehydrogenation of cycloalkanes to the corresponding cycloalkenes and dihydrogen in refluxing cycloalkane (about 200 °C).[7]

These experiments raise several important questions about the mechanism of dehydrogenation. First, does the similarity of the Cp*Ir(PMe$_3$)(CH$_3$)$^+$ complex and the (PCP)Ir(H)$_2$ complex suggest that the dehydrogenation of alkanes proceeds through oxidative addition, reductive elimination, and β-H transfer steps in both systems? Second, given this resemblance what is unique about the (PCP)Ir(H)$_2$ system; why is it catalytic, while the Cp*Ir(PMe$_3$)(CH$_3$)$^+$ system is not?

[†] Present address: Environ. Tech. Div., Pacific Northwest National Laboratory, Richland, WA 99352.

(1) (a) *Transition Metal Hydrides*; Dedieu, A., Ed.; VCH Publishers: New York, 1992. (b) Crabtree, R. H. *The Organometallic Chemistry of the Transition Metals*; John Wiley & Sons: New York, 1988. (c) Arndtsen, B. A.; Bergman, R. G.; Mobley, T. A.; Peterson, T. H. *Acc. Chem. Res.* **1995**, *28*, 154.

(2) (a) Atkins, P. W. *Physical Chemistry*; Oxford University Press: New York, 1990. (b) NIST Standard Reference Database Number 69, 1996, http://webbook.nist.gov/chemistry/.

(3) Burk, M. J.; Crabtree, R. H.; McGrath, D. V. *J. Chem. Soc., Chem. Commun.* **1985**, 1829.

(4) (a) Crabtree, R. H.; Mihelcic, J. M.; Quirk, J. M. *J. Am. Chem. Soc.* **1979**, *101*, 7738. (b) Baudry, M. J.; Ephritikine, M.; Felkin, H.; Holmes-Smith, R. *J. Chem. Soc., Chem. Commun.* **1983**, 788. (c) Baudry, Crabtree, R. H.; Parnell, C. P.; Uriarte, R. J. *Organometallics* **1984**, *3*, 816.

(5) (a) Arndtsen, B. A.; Bergman, R. G. *Science* **1995**, *270*, 1970. (b) Burger, P.; Bergman, R. G. *J. Am. Chem. Soc.* **1993**, *115*, 10462. (c) For a review see: Lohrenz, J. C. W.; Hacobsen, H. *Angew. Chem., Int. Ed. Engl.* **1996**, *35*, 1305.

(6) (a) Strout, D.; Zarić, S.; Niu, S.-Q.; Hall, M. B. *J. Am. Chem. Soc.* **1996**, *118*, 6068. (b) Su, M.-D.; Chu, S.-Y. *J. Am. Chem. Soc.* **1997**, *119*, 5373. (c) Niu, S.-Q.; Strout, D.; Zarić, S.; Bayse, C. A.; Hall, M. B. *ACS Symposium Series*. In press. (d) Niu, S.-Q.; Hall, M. B. *J. Am. Chem. Soc.* **1998**, *120*, 6169. (e) Han, Y.-Z.; Deng, L.-Q.; Ziegler, T. *J. Am. Chem. Soc.* **1997**, *119*, 5939.

(7) (a) Xu, W.-W.; Rosini, G. P.; Gupta, M.; Jensen, C. M.; Kaska, W. C.; Krogh-Jespersen, K.; Goldman, A. S. *J. Chem. Soc., Chem. Commun.* **1997**, 2273. (b) Jensen, C. M.; Gupta, M.; Hee, A.; Hagen, C.; Hoffmann, S.; Kaska, W. C.; Pak, E.; Zidan, R. 215th National Meeting of the American Chemical Society, Dallas, TX, March 29, 1998; Div. Inorg. Chem. Paper 11. (c) Lee, D. W.; Kaska, W. C.; Jensen, C. M. *Organometallics* **1998**, *17*, 1. (d) Gupta, M.; Hagen, C.; Kaska, W. C.; Cramer, R. E.; Jensen, C. M. *J. Chem. Soc., Chem. Commun.* **1996**, 2083. (e) Gupta, M.; Hagen, C.; Kaska, W. C.; Cramer, R. E.; Jensen, C. M. *J. Am. Chem. Soc.* **1997**, *119*, 840. (f) Gupta, M.; Kaska, W. C.; Jensen, C. M. *J. Chem. Soc., Chem. Commun.* **1997**, 461.

10.1021/ja981314d CCC: $18.00
Published on Web 04/07/1999

Here, we explore the catalytic mechanism of alkane dehydrogenation by the model systems $(PCP')Ir(H)_2$ [PCP′ = η^3-$C_6H_3(CH_2PH_2)_2$-1,3] and $CpIr(PH_3)(H)^+$ and the factors responsible for the similarities and differences of their reactions. The geometries and energies of the reactants, intermediates, transition states (TS), and products are determined by the DFT method.

Computational Details

The geometries were optimized with density functional theory (DFT),[8] specifically the Becke three-parameter hybrid exchange functional[9] and the Lee−Yang−Parr correlation functional[10] (B3LYP). The transition states (TS) were optimized by a quasi-Newton method,[11] in which the final updated Hessian shows only one negative eigenvalue, and were characterized by one and only one imaginary frequency for every unique TS in a separate calculation.[12] The basis set for Ir is a modified version of Gaussian 94's[13] LANL2DZ basis,[14] where the two outermost p functions have been replaced by a (41) split of the optimized Ir 6p function from Couty and Hall.[15] The Hay and Wadt double-ζ basis set with effective core potentials[15a] (ECP) was modified for phosphorus by adding a d-type polarization function.[15b] The carbons and hydrogens are described by the Dunning−Huzinaga full double-ζ basis functions with polarization functions (D95**) except for the uncoordinated carbon and hydrogen atoms in the PCP′ ligand [PCP′ = η^3-$C_6H_3(CH_2PH_2)_2$-1,3], where the STO-3G basis set was used,[13] and in the Cp ligand, where the D95 basis set was used. Our previous work has shown that accurate DFT binding energies of transition-metal to ligand bonds require polarization functions on ligand atoms.[6d] The association energies of methane and ethylene with the iridium complexes have been corrected for the basis-set superposition error (BSSE).[16] Although the overall zero-point energy (ZPE) correction of this catalytic reaction is about 8 kcal/mol, these corrections were not included because the differences are not significant for a comparison of the two dehydrogenation systems.

In previous theoretical work on the related $CpIr(PH_3)(CH_3)^+$ system,[6c] we have shown (i) that the oxidative-addition from $CpIr(PH_3)(CH_3)$-(agostic-alkane)$^+$ through an OA/RE transition state (TS) to $CpIr(PH_3)$-$(CH_3)(H)(alkyl)^+$ is endothermic by 4.4 and 0.8 kcal/mol with a low barrier of 11.5 and 10.0 kcal/mol at the DFT-B3LYP and coupled cluster with singles and doubles (CCSD) levels of theory, respectively, (ii) that the reductive-elimination from $CpIr(PH_3)(CH_3)(H)(alkyl)^+$ through an OA/RE TS to a β-agostic complex, $CpIr(PH_3)(alkyl)^+$, is exothermic with a low barrier of 7.1 and 9.2 kcal/mol, and (iii) that β-H transfer from $CpIr(PH_3)(alkyl)^+$ to $CpIr(PH_3)(H)(olefin)^+$ is exothermic by 12 and 16 kcal/mol with a very low barrier of 0.4 and 0.7 kcal/mol. The similarity of the DFT and CCSD results gives us confidence that DFT results will be sufficiently accurate for the comparisons reported here.

All DFT calculations were performed with GAUSSIAN94 programs,[13] at the Supercomputer Facility of Texas A&M University and the Department of Chemistry on Silicon Graphics Power Challenge and the Cray J90 servers, and on Silicon Graphic Power Indigo II IMPACT 10000 workstations in our laboratory.

Scheme 1

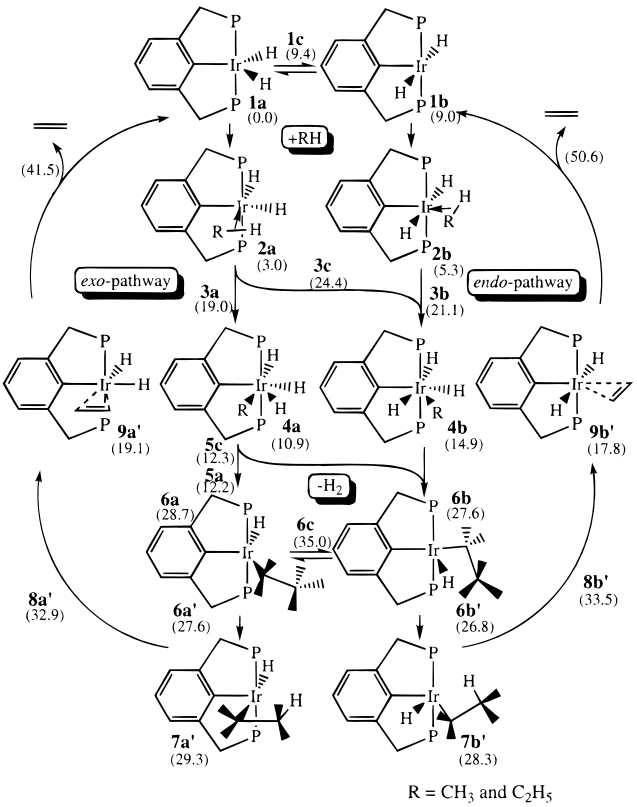

Results and Discussion

The B3LYP method calculates the dehydrogenation reaction 2 to be endothermic by 41.5 kcal/mol with a huge activation barrier of 130.2 kcal/mol. After zero-point energy (ZPE) corrections, the reaction energy and activation barrier for reaction 2 are reduced to 33.0 and 123.9 kcal/mol, respectively. The former value is nearly identical with the accepted experimental value.[7]

$$C_2H_6 \rightarrow C_2H_4 + H_2 \qquad (2)$$

A catalyst reduces the reaction barrier but does not, of course, reduce the endothermicity so that potential catalysts for this reaction often stop with the formation of an olefin complex, unless the reaction is driven by UV irradiation or a hydrogen acceptor.

Since both systems under consideration here, $(PCP')Ir(H)_2$ and $CpIr(PH_3)(H)^+$, are Ir(III) systems, one might expect some similarity in their reaction steps. For the related cationic system, $Cp^*Ir(PMe_3)(CH_3)^+$, the alkane dehydrogenation to alkene is achieved through three important stages: (i) an alkane C−H bond is activated through an oxidative-addition step, (ii) methane is reductively eliminated to form a β-agostic alkyl complex, and (iii) an alkyl β-H transfers to the metal to generate the olefin complex.[6] Here, DFT-B3LYP calculations are used to elucidate the similarities and differences between the potentially catalytic model complexes $(PCP')Ir(H)_2$ and $CpIr(PH_3)(H)^+$.

Alkane Dehydrogenation by $(PCP')Ir(H)_2$ (1). Two possible pathways for the alkane dehydrogenation reaction by (PCP')-$Ir(H)_2$ [PCP′ = η^3-$C_6H_3(CH_2PH_2)_2$-1,3] are shown in Scheme 1. $(PCP')Ir(H)_2$ exists as two isomers **1a** and **1b**, which differ

(8) Parr, R. G.; Yang, W. *Density-functional theory of atoms and molecules*; Oxford University Press: Oxford, 1989.

(9) (a) Becke, A. D. *Phys. Rev.* **1988**, *A38*, 3098. (b) Becke, A. D. *J. Chem. Phys.* **1993**, *98*, 1372. (c) Becke, A. D. *J. Chem. Phys.* **1993**, *98*, 5648.

(10) Lee, C.; Yang, W.; Parr, R. G. *Phys. Rev.* **1988**, *B37*, 785.

(11) Schlegel, H. B. *Theor. Chim. Acta* **1984**, *66*, 33.

(12) Foresman, J. B.; Frish, Æ. *Exploring Chemistry with Electronic Structure. Methods*; Gaussian, Inc.: Pittsburgh, PA 1993.

(13) Frisch, M. J.; Trucks, G. W.; Schlegel, H. B.; Gill, P. M. W.; Johnson, B. G.; Robb, M. A.; Cheeseman, J. R.; Keith, T. A.; Petersson, G. A.; Montgomery, J. A.; Raghavachari, K.; Al-Laham, M. A.; Zakrzewski, V. G.; Ortiz, J. V.; Foresman, J. B.; Cioslowski, J.; Stefanov, B. B.; Nanayakkara, A.; Challacombe, M.; Peng, C. Y.; Ayala, P. Y.; Chen, W.; Wong, M. W.; Andres, J. L.; Replogle, E. S.; Gomperts, R.; Martin, R. L.; Fox, D. J.; Binkley, J. S.; Defrees, D. J.; Baker, J.; Stewart, J. P.; Head-Gordon, M.; Gonzalez, C.; Pople, J. A. Gaussian 94 (Revision D.2); Gaussian, Inc.: Pittsburgh, PA, 1995.

(14) LANL2DZ: Dunning D95 basis sets on first row, Los Alamos ECP plus double-ζ basis sets on Na−Bi.

(15) (a) Hay, P. J.; Wadt, W. R. *J. Chem. Phys.* **1985**, *82*, 299. (b) Couty, M.; Hall, M. B. *J. Comput. Chem.* **1996**, *17*, 1359.

(16) (a) Davidson, E. R.; Feller, A. *Chem. Rev.* **1986**, *86*, 681. (b) *Ab Initio Methods in Quantum Chemistry, Part I*; Lawley, K. P., Ed.; John Wiley & Sons: New York, 1987.

primarily in the H—Ir—H angle. The *exo*-pathway begins with **1a**, while the *endo*-pathway begins with **1b**. Both pathways proceed from alkane OA and H_2 RE through alkyl β-H transfer and olefin elimination. We will consider and examine these two reaction processes separately although we will connect the two paths at appropriate points. Since the alkane ligand has little influence on the OA/RE energy profiles (*vide infra*), methane is used as the reactant in the reaction's early stages (from **1** to **4**) to reduce the calculated system size.

For the reaction mechanism of (PCP′)Ir(H)$_2$ (**1a**−**b**), B3LYP geometry optimizations have been carried out for reactants (**1a**−**b** and CH_4), intermediates (**2a**−**b**, **4a**−**b**, **5a**−**b**, **6a**−**b**, and **18a**−**b**), transition states (**1c**, **3a**−**c**, and **7a**−**b**), and products (**1a**−**b**, C_2H_4, and H_2). Stationary points of the OA/RE and β-H transfer processes along the *exo*- and *endo*-pathways are shown in Figures 1 and 2. Relative energies are summarized in Table 1 (reactions A and B) and Table 2 (reactions C and D), as well as Scheme 1.

The *cis*-dihydride complex **1a**, which has a small H—Ir—H angle (62.7°), is more stable by 9.0 kcal/mol than the *trans*-dihydride complex **1b**, which has a larger H—Ir—H angle (176.6°). The optimized geometry of **1a** corresponds to a highly distorted trigonal bipyrimidal metal center (Y-shaped), while **1b** resembles an octahedral metal center (T-shaped). The largest changes in bond distance from **1a** to **1b** occur for the Ir—C (−0.089 Å) and Ir—H (+0.082 Å) bonds. The conversion from **1a** to **1b** requires a barrier of 9.4 kcal/mol. The TS **1c** displays an unsymmetrical structure where the Ir—H(1) bond and C—Ir—H(1) bond angle are 1.646 Å and 79.9°, while the Ir—H(2) bond and C—Ir—H(2) bond angle are 1.689 Å and 112.5°, respectively. Since the symmetric transformation from a Y-shaped structure to a T-shaped one would involve an orbital crossing between occupied and empty orbitals, the path for interconversion goes through a distorted Y-shaped TS instead of through a trigonal bipyramidal TS.[17]

In comparison to free methane, the longer C—H bonds (+0.022 and +0.026 Å) of both **2a** and **2b** are typical of an α-agostically bound alkane. The transition states **3a**−**c** and oxidative-addition intermediates **4a**−**b** show common pentagonal bipyrimidal structural features, and they have longer Ir—C and Ir—H bonds with respect to the iridium(III) complex, **1a**. The reaction along the *exo*-pathway from **1a** to **2a** and then through the oxidative-addition TS **3a** or **3b** to the oxidative-addition intermediates **4a** or **4b** is endothermic by 10.9 and 14.9 kcal/mol with barriers of 19.0 and 24.4 kcal/mol, respectively. The reaction along the *endo*-pathway from **1a** through **1b** to **2b**, and then through the oxidative-addition TS **3c** to **4b** is endothermic by 14.9 kcal/mol with a barrier of 21.1 kcal/mol.

The dihydride elimination reactions from **4a** or **4b** to **6b** are endothermic by 17.8 and 13.7 kcal/mol, respectively, without any barrier. Here, the dihydrogen associated complexes (between **4a** and **6b** or between **4b** and **6b**) are not observed by the B3LYP calculations because hydride, a stronger *trans* directing ligand, weakens the binding interaction between the metal center and the dihydrogen *trans* to it. In contrast, on the *exo*-pathway the dihydrogen complex, **5a**, is stable because the dihydrogen is *trans* to the carbon of PCP′. The dihydride elimination reaction from **4a** through the TS **5c** to the dihydrogen associated complex **5a** is slightly endothermic by 1.4 kcal/mol with a small barrier of 0.1 kcal/mol. Overall, the dihydride elimination reaction from **5a** to **6a** is endothermic by 16.5 kcal/mol, whereas the dihydride elimination reaction from **4b** to **6b** is endothermic by 12.6 kcal/mol. Since the OA intermediate **4a** is more stable by −4.1 kcal/mol than **4b** and both reactions along the *endo*- and *exo*-pathways have a similar OA barrier (16 kcal/mol), the reaction in the OA/RE stage thermodynamically favors the *exo*-pathway over the *endo*-pathway.

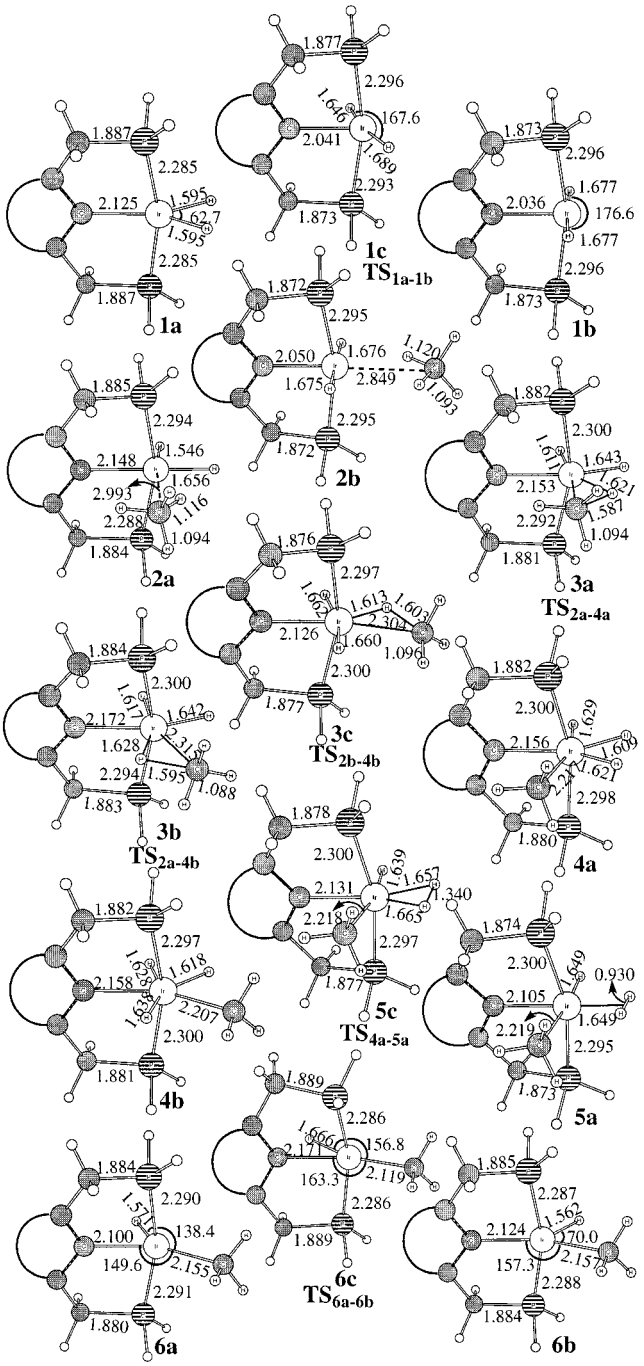

Figure 1. The B3LYP optimized geometries for methane C—H bond activation by the iridium complex along the *exo*- and *endo*-pathways from the reactant, **1a**−**b**, through the intermediates, **2a**−**b**, **4a**−**b**, **5a**, and the transition states, **1c**, **3a**−**c**, **5c**, **6c**, to the dihydride dissociated iridium methyl complexes, **6a**−**b**.

The optimized geometries and relative energies of the Ir methyl complexes and the Ir ethyl complexes show very small differences, where the relative energy differences between **6a** and **6a′** and between **6b** and **6b′** are only 1 kcal/mol. Thus, the calculated results by the simplified models for the OA/RE stage of the reactions are reasonable. Like **6a** and **6b**, the optimized geometries of **6a′** and **6b′** do not show an α-agostic interaction

(17) Riehl, J.-F.; Yves, J.; Eisenstein, O.; Pélissier, M. *Organometallics* **1992**, *11*, 729.

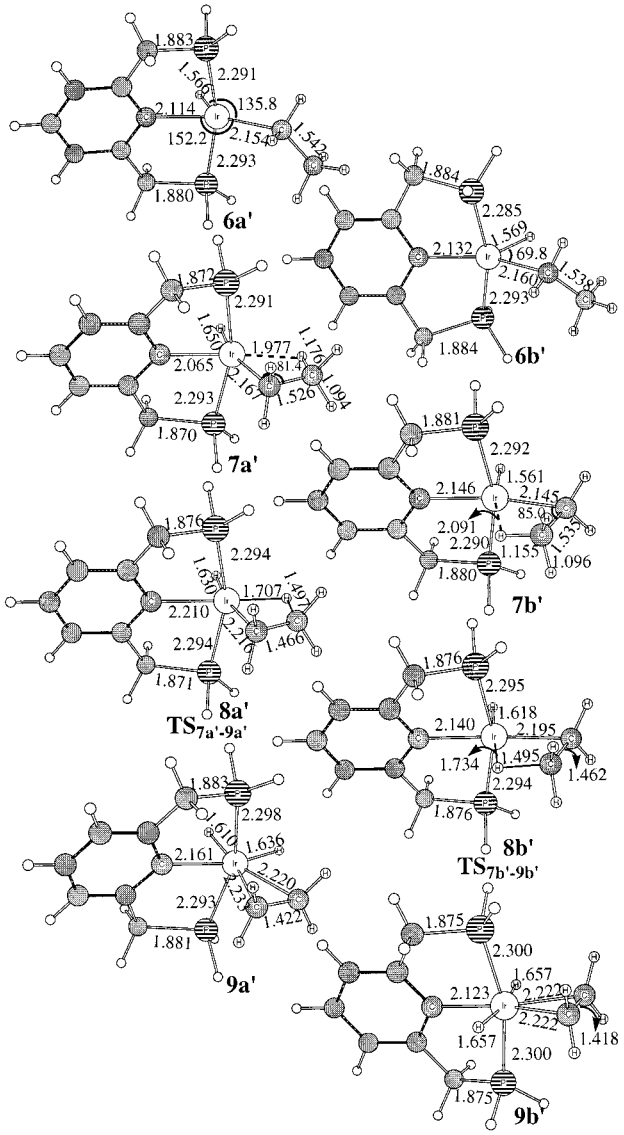

Figure 2. The B3LYP optimized geometries for ethane dehydrogenation by the iridium complex along the *exo*- and *endo*-pathways from the reactant, **1a**−**b**, through the intermediates, **6a′**−**b′**, **7a′**−**b′**, and the transition states, **8a′**−**b′**, to the iridium olefin π-complexes, **9a′**−**b′**.

between the ethyl C^{α}—H bond and metal center. As the ethyl ligand of **6a′** and **6b′** rotates, the complexes **7a′** and **7b′** form, which have very strong β-agostic interactions. In **7a′** and **7b′**, the C^{β}—H bond and the Ir—C^{α}—C^{β} angle are shorter and smaller than the values of normal C—H bonds and sp^3 hybrid angles (109.5°). Similar relative energies between **6a′** and **7a′** and between **6b′** and **7b′** show that there is significant strain in the β-agostic structures.

From the β-agostic structures (**7a′**−**b′**), the reaction proceeds toward the β-H transfer through a four-center transition state, **8a′**−**b′**, where the Ir—H bond is being formed and the inside C^{β}—H bond is being broken. The small geometrical differences between **7a′** and **8a′** and between **7b′** and **8b′** point to a very early transition state. In the β-H transfer products, the olefin dihydride complexes **9a′**−**b′**, the Ir—C (olefin) distances are fairly short, only about 0.06 Å longer than the Ir—C (ethyl) distances of **6a′**−**b′**. Furthermore, the C═C bond distances of **9a′**−**b′**, about 1.42 Å, are clearly longer by 0.08 Å than that of a free ethylene. Thus, as in the $CpIr(PH_3)(CH_3)(\eta^2\text{-ethylene})^+$ complex,[6c] the Ir—ethylene bonds of the $(PCP')Ir(H)_2(\eta^2$-ethylene) complexes, **9a′**−**b′**, are fairly covalent, which results in Ir(V)-like characteristics.

Table 1. B3LYP Relative Energies (kcal/mol) of the Methane C—H Activation Reactions

structure		ΔE^a
A: The Methane C—H Activation Reaction by $(PCP')Ir(H)_2$ (*exo*-Pathway)		
$(PCP')Ir(H)_2$, CH_4	**1a** + methane	0.00
$(PCP')Ir(H)_2(CH_4)$	**2a**	3.03
$(PCP')Ir(H)_2(H)(CH_3)$	**3a (TS$_{2a-4a}$)**	19.03
$(PCP')Ir(H)_2(H)(CH_3)$	**4a**	10.86
$(PCP')Ir(H)_2(H)(CH_3)$	**5c (TS$_{4a-5a}$)**	12.31
$(PCP')Ir(H_2)(H)(CH_3)$	**5a**	12.22
$(PCP')Ir(H)(CH_3)$, H_2	**6a** + H_2	28.68
$(PCP')Ir(H)(CH_3)$, H_2	**6c** + H_2 **(TS$_{6a-6b}$)**	34.96
B: The Methane C—H Activation Reaction by $(PCP')Ir(H)_2$ (*endo*—Pathway)		
$(PCP')Ir(H)_2$, CH_4	**1c** + methane **(TS$_{1a-1b}$)**	9.43
$(PCP')Ir(H)_2$, CH_4	**1b** + methane	9.02
$(PCP')Ir(H)_2(CH_4)$	**2b**	5.33
$(PCP')Ir(H)_2(H)(CH_3)$	**3b (TS$_{2b-4b}$)**	21.14
$(PCP')Ir(H)_2(H)(CH_3)$	**3c (TS$_{2a-4b}$)**	24.35
$(PCP')Ir(H)_2(H)(CH_3)$	**4b**	14.94
$(PCP')Ir(H)(CH_3)$, H_2	**6b** + H_2	27.57

[a] The BSSE correction is included.

Table 2. B3LYP Relative Energies (kcal/mol) of the Ethane C—H Activation Reactions

structure		ΔE^a
C: The Ethane C—H Activation Reaction by $(PCP')Ir(H)_2$ (*exo*-Pathway)		
$(PCP')Ir(H)_2$, C_2H_6	**1a** + ethane	0.00
$(PCP')Ir(H)(C_2H_5)$, H_2	**6a′** + H_2	27.62
$(PCP')Ir(H)(C_2H_5)$, H_2	**7a′** + H_2	29.30
$(PCP')Ir(H)(H)(C_2H_4)$, H_2	**8a′** ($TS_{7a'-9a'}$)	32.88
$(PCP')Ir(H)(H)(C_2H_4)$, H_2	**9a′**	19.14
$(PCP')Ir(H)_2$, H_2, C_2H_4	**1a** + H_2 + C_2H_4	41.53
D: The Ethane C—H Activation Reaction by $(PCP')Ir(H)_2$ (*endo*-Pathway)		
$(PCP')Ir(H)(C_2H_5)$, H_2	**6b′** + H_2	26.75
$(PCP')Ir(H)(C_2H_5)$, H_2	**7b′** + H_2	28.29
$(PCP')Ir(H)(H)(C_2H_4)$, H_2	**8b′** ($TS_{7b'-9b'}$)	33.45
$(PCP')Ir(H)(H)(C_2H_4)$, H_2	**9b′**	17.83
$(PCP'')Ir(H)_2$, H_2, C_2H_4	**1b** + H_2 + C_2H_4	50.55

[a] The BSSE correction is included.

The β-H transfer reaction from **7a′** through **8a′** to **9a′** is exothermic by 10.2 kcal/mol with a barrier of 3.6 kcal/mol, while the corresponding reaction from **7b′** through **8b′** to **9b′** is exothermic by 10.5 kcal/mol with a barrier of 5.2 kcal/mol. Since the reverse reaction, the olefin insertion reaction, from **9** to **7**, is more favorable than the olefin C—H bond activation (Scheme 2, reaction A) to an oxidative-addition intermediate,[6c] it is likely that the deuterium exchange reaction (3)[7b,c] proceeds through the olefin insertion process (Scheme 2, reaction B).

$$H_2C{=}CRH \xrightarrow{(PCP)Ir(D)_2} HDC{=}CRH \qquad (3)$$

The olefin dissociation energy from **9a′** to **1a** + C_2H_4 is 22.4 kcal/mol, which is 10.3 kcal/mol less than that from **9b′** to **1b** + C_2H_4. For the olefin dissociation from **9b′** directly to **1a**, the lowest possible energy would still be more endothermic by 1.3 kcal/mol than that from **9a′** to **1a**, and the more extensive hydride rearrangement would increase the barrier. Thus, because of the large energy difference in the olefin elimination steps the overall reaction favors the *exo*-pathway over the *endo*-pathway.

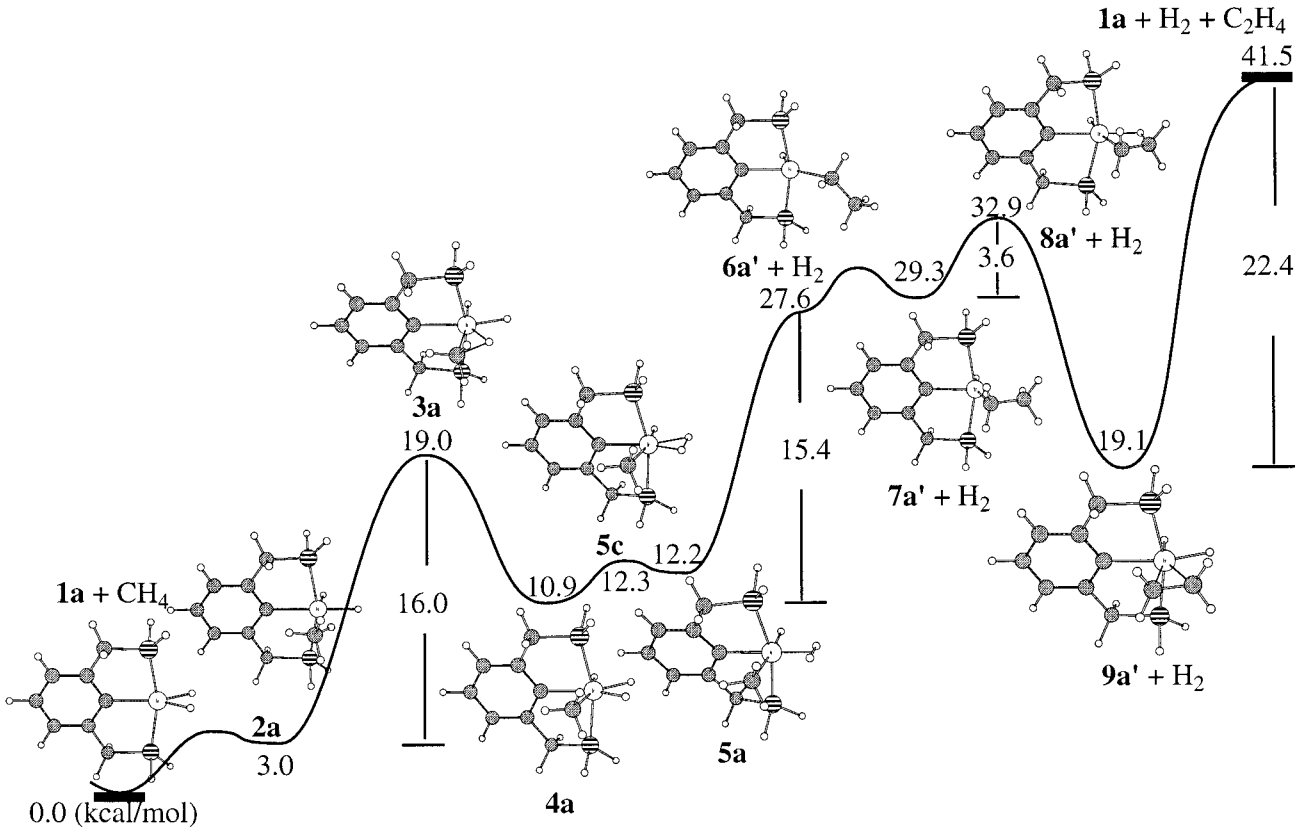

Figure 3. The B3LYP energy profiles of alkane dehydrogenation along the *exo*-pathway from **1a** and methane/ethane to **1a**, H_2, and C_2H_6. In the OA/RE reaction stage, the energy numbers are relative to the total energy of reactants, **1a** and CH_4. In the β-H transfer reaction stage, the energy numbers are relative to the total energy of reactants, **1a** and C_2H_6.

Scheme 2

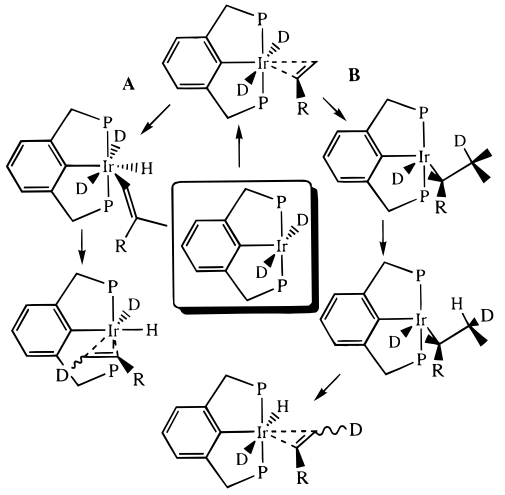

The stationary points and energy profiles along the *exo*-pathway are shown in Figure 3. The last step (**9a′** → **1a**) appears to be the rate-determining step. In the course of this reaction other species not on the most direct path shown in Figure 3 may be formed but they must eventually return to **9a′** before they produce product (see Scheme 1). The most viable alternative path to **9a′** proceeds through **4b** rather than **4a** to **6b** then to **6a**. Clearly, the critical steps of the (PCP′)Ir(H)$_2$ catalyzed dehydrogenation are alkane oxidative addition, dihydride reductive elimination, and olefin dissociation.

Alkane Dehydrogenation by CpIr(PH$_3$)(H)$^+$ (10). For the alkane dehydrogenation reaction by CpIr(PH$_3$)(H)$^+$, shown in Scheme 3, we have carried out B3LYP geometry optimizations for both methane and ethane C—H bond activation reactions.

Scheme 3

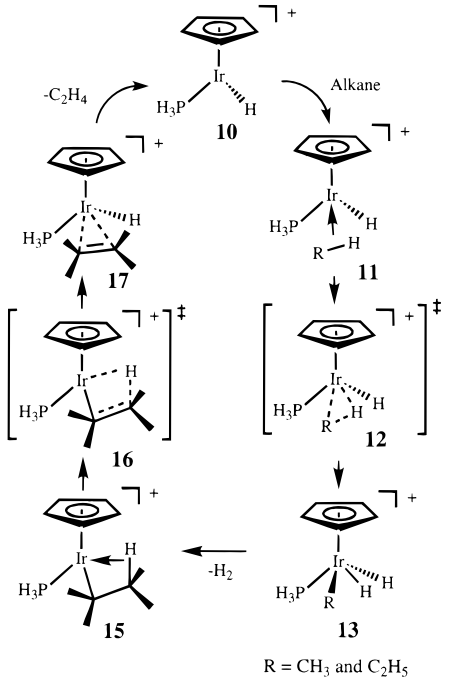

For the ethane C—H bond activation reaction the optimized geometries of the reactants (**10** and C_2H_6) through intermediates (**11′**, **13′**, **15′**, and **17′**), and transition states (**12′** and **16′**), to dihydride-elimination complex (**14′**) are shown in Figure 4. The structures of the methane species from its C—H bond activation reaction, **11**—**14** (see Supporting Information), are quite similar

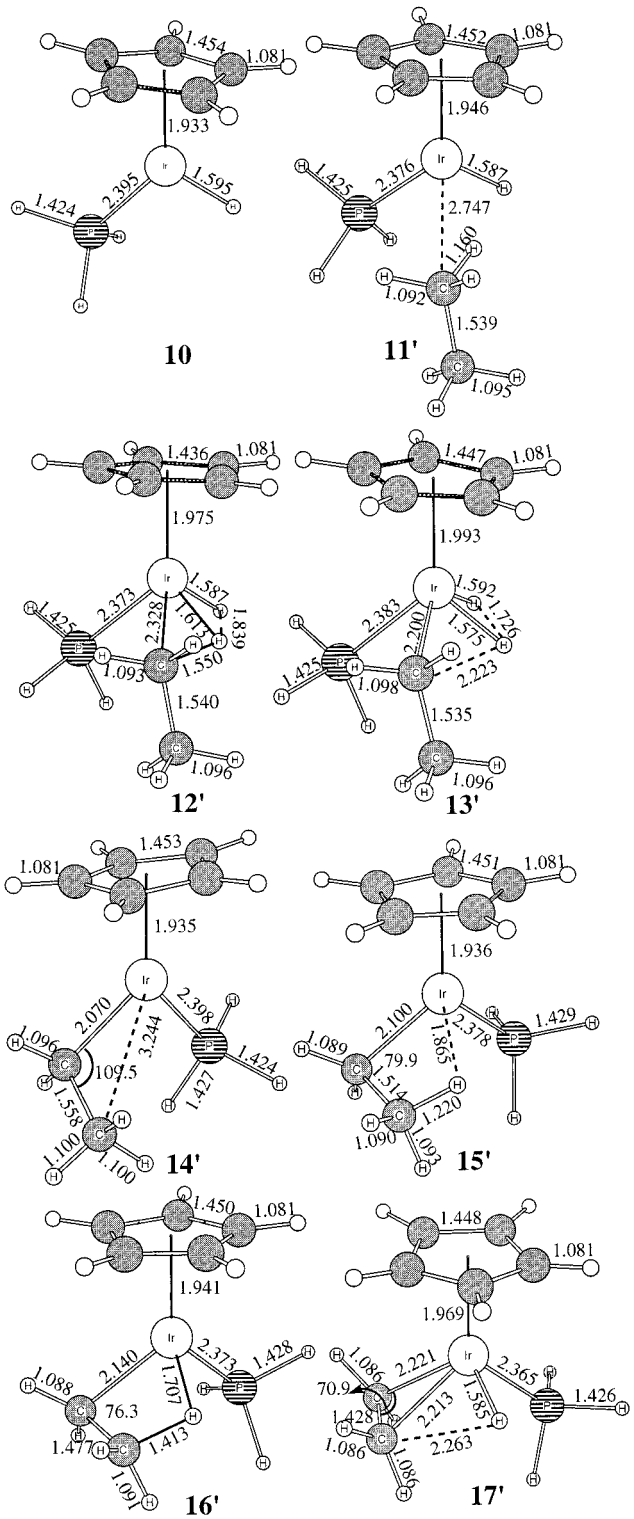

Figure 4. The B3LYP optimized geometries for ethane dehydrogenation by the iridium complex from the reactant, **10**, through the α-agostic complex, **11′**, the OA transition state, **12′**, to the OA intermediate, **13′**, and then through the dihydride dissociated iridium ethyl complex, **14′**, the *β*-agostic iridium complex, **15′**, and the *β*-H transfer transition state, **16′**, to the olefin *π*-complex, **17′** (only the average C—C and C—H distances are given for the Cp ring).

to the corresponding ethane species, **11′**−**14′**. The energies of these species can be compared in Table 3 (reactions E and F).

Methane and ethane are bound to the $CpIr(PH_3)(H)^+$ complex in an agostic fashion by −7.8 and −9.7 kcal/mol, respectively (**11**, **11′**). The stronger binding of ethane is consistent with our previous work.[6c,18] The barrier to C—H bond activation is similar, 8.3 and 9.0 kcal/mol for methane and ethane, respectively. For ethane, the OA intermediate (**13′**) is slightly less stable by 2.1 kcal/mol than its agostic complex (**11′**), whereas for methane, the OA intermediate (**13**) is isoenergetic (differs by less than 0.5 kcal/mol) to its agostic complex (**11**). The similarities described here support our replacement of ethane by methane to simplify some aspects of the computational models.

Table 3. B3LYP Relative Energies (kcal/mol) of the Ethane and Methane C—H Activation Reactions (E and F)

structure		ΔE^a
E: The Ethane Dehydrogenation by $CpIr(PH_3)(H)^+$		
$CpIr(PH_3)(H)^+$, C_2H_6	**10** + ethane	0.00
$CpIr(PH_3)(H)(C_2H_6)^+$	**11′**	−9.68
$CpIr(PH_3)(H)(H)(C_2H_5)^+$	**12′ ($TS_{11'-13'}$)**	−0.73
$CpIr(PH_3)(H)(H)(C_2H_5)^+$	**13′**	−7.61
$CpIr(PH_3)(C_2H_5)^+$, H_2	**14′** + H_2 **($TS_{13'-15'}$)**	16.72
$CpIr(PH_3)(C_2H_5)^+$, H_2	**15′** + H_2	12.92
$CpIr(PH_3)(H)(C_2H_4)^+$, H_2	**16′** + H_2 **($TS_{15'-17'}$)**	13.64
$CpIr(PH_3)(H)(C_2H_4)^+$, H_2	**17′** + H_2	0.73
$CpIr(PH_3)(H)^+$, H_2, C_2H_4	**10** + H_2 + C_2H_4	41.53
F: The C—H Activation Reaction of Methane		
$CpIr(PH_3)(H)^+$, CH_4	**10** + methane	0.00
$CpIr(PH_3)(H)(CH_4)^+$	**11**	−7.76
$CpIr(PH_3)(H)(H)(CH_3)^+$	**12 (TS_{11-13})**	0.51
$CpIr(PH_3)(H)(H)(CH_3)^+$	**13**	−7.64
$CpIr(PH_3)(CH_3)^+$, H_2	**14** + H_2	16.60

[a] The BSSE correction is included.

For methane, the reactions with $CpIr(PH_3)(H)^+$ (**10**) (reaction E) are similar to those reported previously[6c] for $CpIr(PH_3)(CH_3)^+$ (**14**). However, **10** binds methane more strongly to form **11** than **14** binds methane to form $CpIr(PH_3)(CH_3)(CH_4)^+$ ($\Delta\Delta E = -6.7$ kcal/mol). The OA intermediate (**13**) is likewise more stable than the corresponding species for $CpIr(PH_3)(CH_3)^+$, where the reaction energy from the reactants **10** and methane to **13** is −7.6 kcal/mol, while the reaction energy from the reactants **14** and methane to $CpIr(PH_3)(CH_3)_2(H)^+$ is +3.4 kcal/mol. In the reductive elimination step from **13** to **14** and H_2, dihydrogen is not bound, unlike methane which has a weak agostic bound to **14**. Thus, dihydrogen elimination proceeds endothermically without an additional barrier. The lower activation energies for H—H bond activation compared to those for C—H bond activation are derived, in part, from the ability of the H 1s orbital to simultaneously maintain a large overlap between both the breaking H—H and forming Ir—H bonds. In contrast, the highly directional sp^3 hybrid orbitals on the carbon of alkyl ligands cannot simultaneously maintain such a large overlap during the C—H bond activation.[1a,19] In addition, since Ir—H bonds are stronger than Ir—C bonds, the H—H bond activation is generally more exothermic than the corresponding C—H bond activation.

Since the dihydride reductive-elimination transition state, the dihydrogen associated complex, and the ethyl iridium α-agostic complex are not observed by DFT calculations, the "non-agostic" iridium−ethyl complex, $CpIr(PH_3)(C_2H_5)^+$ (**14′**), where the $Ir—C^{\alpha}—C^{\beta}$ angle is fixed at 109.5° and all other parameters are optimized, was taken as an approximate transition state from **13′** to the *β*-agostic complex **15′** and H_2. The *β*-H transfer

(18) Zarić, S.; Hall, M. B. *J. Phys. Chem. A* **1997**, *101*, 4646.
(19) (a) Hay, P. J. *Transition Metal Hydrides*; Dedieu, A., Ed.; VCH Publishers: New York, 1992; Chapter 4, p 127. (b) Low, J. J.; Goddard, W. A., III *Organometallics* **1986**, *5*, 609. (c) Blomberg, M. R. A.; Brandemark, U.; Siegbahn, P. E. M. *J. Am. Chem. Soc.* **1983**, *105*, 5557. (d) Obara, S.; Kitaura, K.; Morokuma, K. *J. Am. Chem. Soc.* **1984**, *106*, 7482.

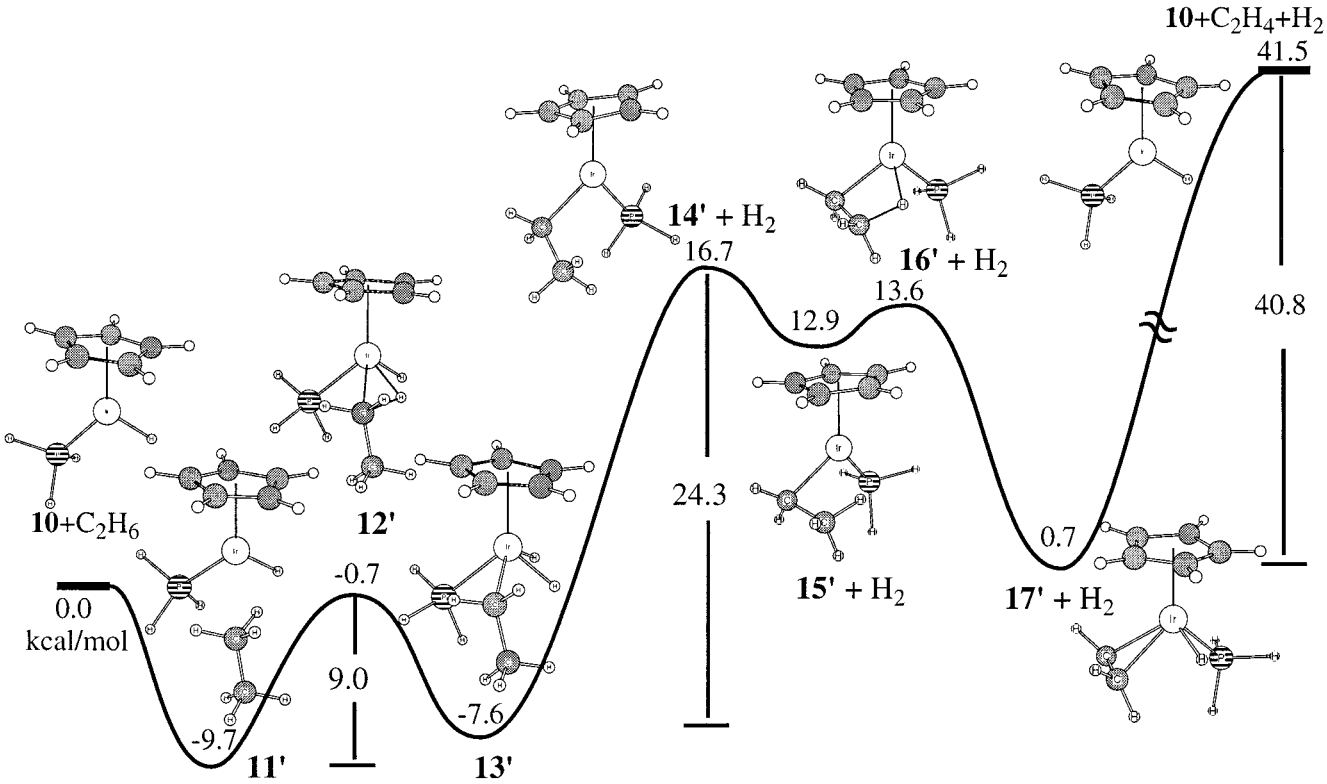

Figure 5. The B3LYP energy profiles of ethane dehydrogenation along the OA/RE and β-H transfer pathways from **10** and C_2H_6 through **11′**−**17′** to **10**, H_2, and C_2H_6.

reaction from **15′** through transition state **16′** to the Ir—olefin π-complex **17′** is exothermic by 12.2 kcal/mol with a very low activation barrier of 0.7 kcal/mol. In previous work,[6c] we have mentioned (i) that the slipped Cp ring in the iridium ethylene π-complex is similar to that found in the Ir(V) OA/RE intermediate, (ii) that ethylene plays such a strong electron acceptor role that it takes on some $C_2H_4^{2-}$ character, and (iii) that the resulting complex has significant Ir(V) character. Thus, $CpIr(PH_3)(\eta^2\text{-}C_2H_4)^+$ (**17′**) has a large ethylene dissociation energy of 40.8 kcal/mol.

Overall, as shown in Figure 5, the ethane dehydrogenation by **10** to the iridium π-complex **17′** and H_2 is slightly endothermic. The rate-determining step in the activation of ethane to form olefin complexes by $CpIr(PH_3)(H)^+$ is the dihydride reductive-elimination step. However, since the olefin dissociation energy from **17′** to **10** + C_2H_4 is 40.8 kcal/mol, olefin elimination becomes the critical step for this complex's catalytic dehydrogenation cycle. The calculated results are consistent with the fact that only intermediates such as **17′** have been observed experimentally and that the catalytic cycle is not completed in the $Cp^*Ir(PMe_3)(R)^+$ system.

Comparison of $CpIr(PH_3)(H)^+$ and $(PCP')Ir(H)_2$ Systems. The calculated results suggest that alkane dehydrogenation by $(PCP)Ir(H)_2$ and $Cp^*Ir(PMe_3)(R)^+$ proceeds through similar reaction intermediates and TS. Although the alkane OA reaction for $CpIr(PH_3)(H)^+$ has a lower barrier (lower by 7 kcal/mol) than that for $(PCP')Ir(H)_2$, the dihydride and olefin elimination reactions have much higher barriers (higher by 9 and 19 kcal/mol, respectively). The unbalanced barriers of the alkane dehydrogenation by $CpIr(PH_3)(H)^+$ finally lead to the reaction terminating at **17′**. The $(PCP')Ir(H)_2$ system is special because it balances these three barriers (the alkane OA, dihydride RE, and olefin elimination) such that they are energetically quite similar (16, 15, and 22 kcal/mol, respectively, for our model $(PCP')Ir(H)_2$). Clearly, the balance of these three barriers depends on the stabilizing interaction between metal center and ligand in the Ir(V) complexes, **4a**−**b** and **13′**, and the π-complexes, **9a′**−**b′** and **17′**. Thus, the electronic effect of the ligands plays an important role in these Ir(III) alkane dehydrogenation reactions.

It is well-known that the ease of alkane C—H bond activation and the strength of metal—olefin bonds depend, in part, on the energy differences between the singlet and triplet states (ΔE_{T-S}) of the transition-metal fragment.[6b,20] For example, third-transition-row metal complexes undergo oxidative addition, $M^I + A{-}B \rightarrow M^{III}(A)(B)$, more easily than their second-transition-row metal congeners because late third-transition-row metals have either d^ns^1 ground states or d^ns^1 low-lying excited states, while late second-transition-row metals have d^{n+1} ground states with high-lying d^ns^1 excited states.[20,21] This rationale emphasizes the importance of forming sd hybrids for the two new covalent bonds in the product. A corresponding behavior exists in the oxidative-addition reaction studied here, $M^{III} + A{-}B \rightarrow M^V(A)(B)$.[6]

The energy differences between the singlet and triplet states of the $CpIr(PH_3)(H)^+$ and $(PCP')Ir(H)_2$ fragments of **4a**, **9a′**, **13′**, and **17′** are shown in Table 4. These energies are for the unoptimized fragments created by simply removing the (H)(CH$_3$) ligands or the C_2H_4 ligands. From Table 4 one can see that even for geometries corresponding to the removal of a different set of ligands, the $CpIr(PH_3)(H)^+$ fragment consistently has a smaller ΔE_{T-S} than the $(PCP')Ir(H)_2$ fragment. In orbital terms the $CpIr(PH_3)(H)^+$ fragment has a higher-lying occupied d_π orbital and a lower-lying unoccupied d_σ orbital with respect

(20) Jiménez-Cataño, R.; Niu, S.-Q.; Hall, M. B. *Organometallics* **1997**, *16*, 1962.

(21) (a) Low, J. J.; Goddard, W. A., III *J. Am. Chem. Soc.* **1986**, *108*, 6115. (b) Low, J. J.; Goddard, W. A., III *J. Am. Chem. Soc.* **1984**, *106*, 8321. (c) Low, J. J.; Goddard, W. A., III *J. Am. Chem. Soc.* **1984**, *106*, 6928.

Table 4. The Energy Differences (kcal/mol) between the Singlet and Triplet States of the $CpIr(PH_3)(H)^+$ and $(PCP')Ir(H)_2$ Fragments of **13**, **17′**, **4a**, and **9a′**

	$CpIr(PH_3)(H)^+\cdots L\ \Delta E_{T-S}$	$(PCP')Ir(H)_2\cdots L\ \Delta E_{T-S}$
$L = (H)(CH_3)$	7.60	14.17
$L = C_2H_4$	17.33	29.33

Scheme 4

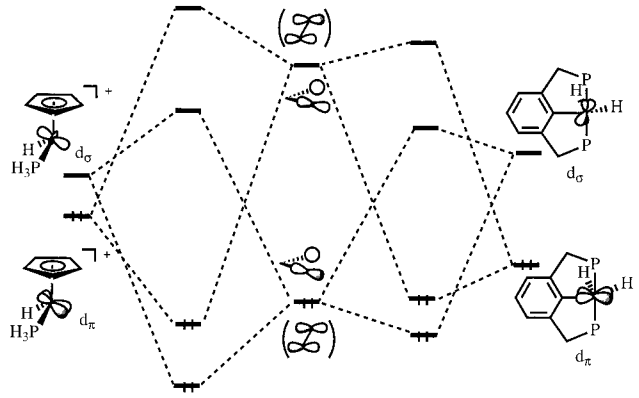

to those of the $(PCP')Ir(H)_2$ fragment. Thus, $CpIr(PH_3)(H)^+$ will stabilize two σ bonds, such as the ligand pair $(H)(CH_3)$, more effectively than $(PCP')Ir(H)_2$. Likewise, $CpIr(PH_3)(H)^+$ will be a better π donor and a better σ acceptor and will form a stronger bond to an alkene or alkyne in the Dewer−Chatt−Duncanson model. Scheme 4 illustrates both cases.

Conclusions

The alkane dehydrogenations by $(PCP')Ir(H)_2$ (**1**) and $CpIr(PH_3)(H)^+$ (**10**) proceed through similar reaction steps: (i) alkane oxidative addition from the agostic complex to the OA intermediate is endothermic by 7.9 and 2.1 kcal/mol with a barrier of 16.0 and 9.0 kcal/mol, respectively, (ii) dihydride reductive elimination is endothermic by 16.7 and 24.3 kcal/mol, respectively, (iii) β-H transfer from the β-agostic complex to the olefin π-complex is exothermic by 10.2 and 12.3 kcal/mol with a low barrier of 3.6 and 0.7 kcal/mol, respectively, and (iv) olefin dissociation is endothermic by 22.4 and 40.8 kcal/mol, respectively. The critical barriers of the $CpIr(PH_3)(H)^+$ and $(PCP')Ir(H)_2$ catalyzed dehydrogenation are alkane oxidative addition, dihydride reductive elimination, and olefin dissociation.

The $(PCP')Ir(H)_2$ system is special because these three barriers are balanced (16, 15, and 22 kcal/mol, respectively), whereas in the $CpIr(PH_3)(H)^+$ system these three barriers are unbalanced (9, 24, and 41 kcal/mol, respectively). Thus, in the catalytic cycle of the alkane dehydrogenation by $(PCP')Ir(H)_2$ the reaction endothermicity is achieved gradually.[22] The higher stabilities of the Ir(V) complex and the π-complex (which has some Ir(V) character) in the $CpIr(PH_3)(H)^+$ system are responsible for these differences in the energy of the critical steps. Our results show that these differences can be traced to the singlet−triplet energy splitting of the metal ligand fragments $(PCP')Ir(H)$ vs $CpIr(PH_3)^+$.

Acknowledgment. This work was supported by the Robert A. Welch Foundation (A-648) and the National Science Foundation (CHE9423271, CHE9528196, and CHE9800184).

Supporting Information Available: The B3LYP optimized geometries for methane C−H bond activation by the iridium complex from the α-agostic complex, **11**, through the OA transition state, **12**, and the OA intermediate, **13**, to the dihydride dissociated iridium methyl complex, **14**, (only the average C−C and C−H distances are given for the Cp ring) (PDF). This material is available free of charge via the Internet at http://pubs.acs.org.

JA981314D

(22) Since neither potential energy surface has a barrier higher than the endothermicity of the reaction, either catalyst would be equally effective in a gas-phase reaction. However, in solution as the intermediates reequilibrate to the temperature of the "bath", each barrier must be overcome independently.